

Interfacial potentials for Al/SiC(111)

This article has been downloaded from IOPscience. Please scroll down to see the full text article.

2009 J. Phys.: Condens. Matter 21 225002

(<http://iopscience.iop.org/0953-8984/21/22/225002>)

View [the table of contents for this issue](#), or go to the [journal homepage](#) for more

Download details:

IP Address: 129.252.86.83

The article was downloaded on 29/05/2010 at 20:04

Please note that [terms and conditions apply](#).

Interfacial potentials for Al/SiC(111)

Hanyue Zhao¹, Nanxian Chen^{1,2} and Yao Long¹

¹ Department of Physics, Tsinghua University, Beijing 100084, People's Republic of China

² Institute for Applied Physics, University of Science and Technology, Beijing 100083, People's Republic of China

E-mail: zhaohy03@mails.tsinghua.edu.cn

Received 28 December 2008, in final form 9 March 2009

Published 22 April 2009

Online at stacks.iop.org/JPhysCM/21/225002

Abstract

To study the metal/semiconductor interface by means of atomistic simulation, an effective interfacial potential is an important issue. In this work, *ab initio* adhesive energies are used to derive interfacial potentials for the Al/SiC(111) interface. In order to describe the directional covalent bonds at the interface, we suggest a potential model comprising both two-body and three-body terms. The former is a parameter-free potential obtained by a lattice inversion method and the latter is assigned in modified Stillinger–Weber potential form. The obtained potentials are used to study the position of misfit dislocations in the Al/SiC(111) interface. There is a coherent Al interlayer on the interface plane and the dislocation appears on the Al side.

(Some figures in this article are in colour only in the electronic version)

1. Introduction

The metal/semiconductor interface is an important issue in semiconductor science and industry, playing a key role in determining the quality of electronic devices. For theoretical studies in this field, an *ab initio* calculation is considered as an accurate method but costly in computational time when dealing with complex atomic systems. In this situation, atomistic simulation based on interatomic potentials is highlighted. However, the determination of potentials for a target system is usually a difficult task. Theoretical effort on this subject is necessary.

In this work, we aim to develop effective interfacial potentials for the Al/SiC(111) interface. SiC is an excellent material with promising applications in electronic devices and Al is one of the most commonly used metals for contact with SiC, so Al/SiC is a widely studied topic both in theory [1–5] and experiment [6–8]. Most of the theoretical works are done by the *ab initio* method [2–4], while atomistic simulations [5] are rather rare. This may be due to the lack of interfacial potentials.

In a view that SiC is a typical covalent compound associated with directional chemical bonds, many-body interactions are introduced in the energy expression. At the metal/SiC interface, where metal atoms terminate the dangling bonds on the SiC surface, many-body interactions are inherited. Previously, we have studied the Al/SiC(100)

interface by a pair-potential model [9] and gotten partial success. But there remains a problem that the transferability of pair potentials is not very good. So we turn to the Al/SiC(111) interface, making an effort to find a description based on both two-body and three-body potentials. The three-body interactions are assigned in modified Stillinger–Weber (MSW) potential form [10, 11], which has been widely used in covalent matters with diamond and zinc blende structures [12–15]. At the metal/SiC(111) interface, the terminated Si or C atoms are in fourfold-coordinated sites [3], indicating an sp^3 orbital hybridization, so the MSW potential is suitable. In addition, the previous work of our group [15] has developed the MSW potential for bulk SiC. A new attempt is made to extend this method now for modeling the metal/SiC interface.

Besides the derivation of interfacial potentials, we use them to study misfit dislocations in the Al/SiC(111) interface. It is known that misfit dislocation is an important issue in mismatched interfaces, which affects many interfacial properties such as adhesive energy, tensile stress, slip stress, etc. The investigation in this work focuses on the dislocation position, trying to get a basic understanding of the misfit-induced interface structure.

The following work is divided into three parts. First, in section 2, the method to obtain interfacial potentials is introduced. Then, in section 3, these potentials are used to study the misfit dislocation. Finally, section 4 is the conclusion.

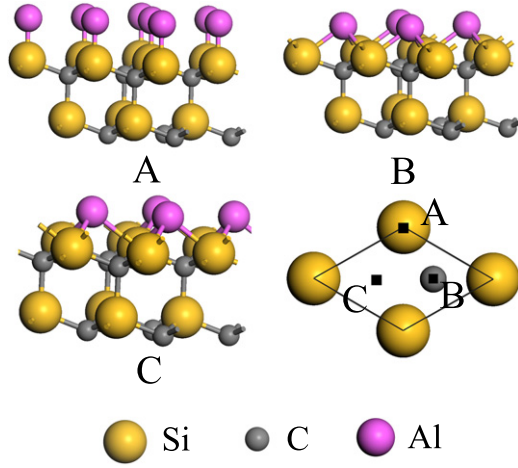


Figure 1. Three atomic configurations of the Al/SiC(111) interface, taking the Si-terminated case as an illustration. The symbols A, B and C refer to top site, hollow site and hex site, respectively. Only a few layers near the interface are presented.

2. Derivation of interfacial potentials

2.1. Interface structures

In this work, *ab initio* adhesive energies (AEs) of some symmetric interface configurations are used as the data source to derive interfacial potentials. So first of all, these interface structures are introduced. As we know, Al/SiC is a mismatched interface with a misfit of 8.3%, obtained by $(a_{\text{SiC}} - a_{\text{Al}})/a_{\text{SiC}}$, where a_{Al} and a_{SiC} are the lattice constants of Al and SiC, respectively. For convenience, coherent interface models are used in *ab initio* calculations, where the Al lattice is forced to match the SiC lattice, since the latter is more rigid than the former.

According to symmetry, there are three representative configurations of the Al/SiC(111) coherent interface, named top-site, hollow-site and hex-site structures, as shown in figure 1. AE is used to measure the adhesion between Al and

SiC, defined as

$$E_{\text{ad}} = \frac{1}{A} (E_{\text{total}} - E_{\text{Al}} - E_{\text{SiC}}), \quad (1)$$

where E_{total} is the total energy of the interface system, E_{Al} and E_{SiC} are the energies of isolated metal and SiC slabs, and A is the interface area. Here E_{ad} is evaluated as a function of interfacial distance x .

Ab initio AEs are calculated by using a CASTEP code [16]. Each computational model consists of six Al monolayers (MLs) and thirteen SiC MLs. The generalized gradient approximation (GGA) is used, with a plane-wave cutoff energy of 400 eV, and the K-point mesh is $7 \times 7 \times 3$.

The results show that top-site structures are energetically preferred for both Si-terminated and C-terminated interfaces, which is in agreement with [3]. The hollow-site and hex-site structures are not so favorable in the energetic view, but still worth paying attention to as they may appear in the misfit dislocation core.

We also investigate the charge transfer at the interface by calculating the difference charge density:

$$\Delta\rho = \rho_{\text{Al/SiC}} - \rho_{\text{SiC}} - \rho_{\text{Al}}, \quad (2)$$

where $\rho_{\text{Al/SiC}}$ is the charge density of the Al/SiC interface, and ρ_{SiC} and ρ_{Al} are those of isolated SiC and Al slabs. The results are displayed in figure 2, showing some unique features. First, the charge transfer at the C-terminated interface is confined to the first SiC and Al layers, while it extends to the second SiC layer at the Si-terminated interface. Second, charge accumulations are localized between the interfacial Al and Si (or C) atoms, implying a typical characteristic of covalent bonds between Al and SiC. So three-body modification in potential modeling is necessary.

2.2. The potential model

In a three-body approximation, the AE can be written as a summation of two-body and three-body interactions:

$$E_{\text{ad}} = \sum_{i,j} \Phi_{ij}(r_{ij}) + \sum_{i,j,k} \Phi_{jik}(r_{ij}, r_{ik}, \theta_{jik}), \quad (3)$$

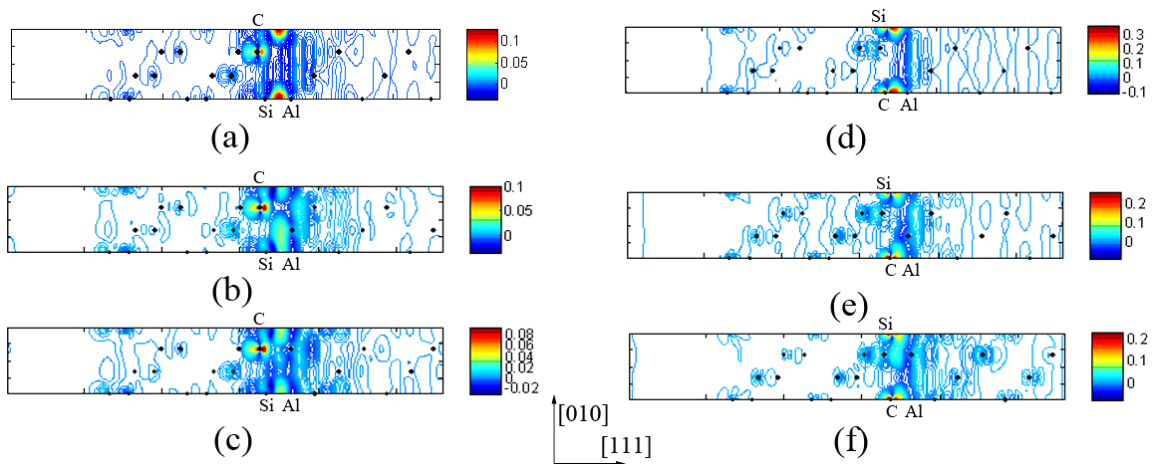


Figure 2. Difference charge densities of Al/SiC(111) interfaces, in units of $e \text{ \AA}^{-3}$. The left column is for Si-terminated interfaces, and the right column is for C-terminated interfaces. (a) and (d), (b) and (e) and (c) and (f) are the contour plots of top-site, hollow-site and hex-site structures, respectively.

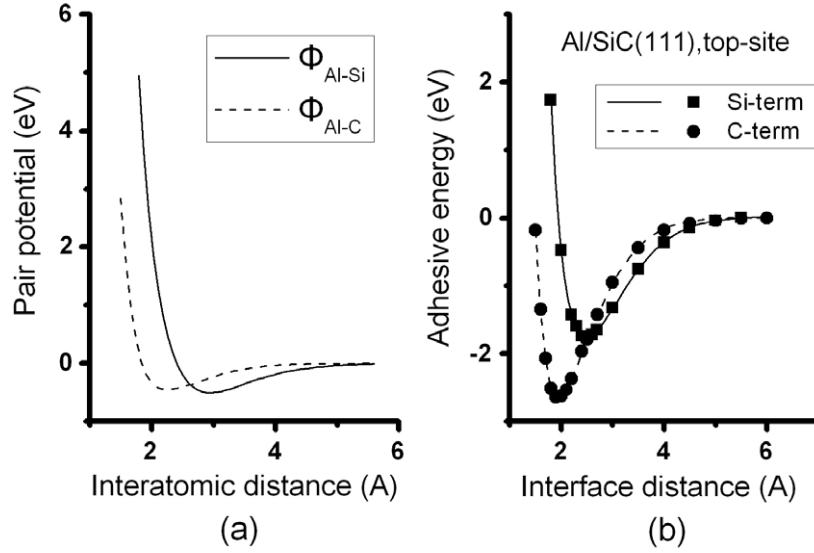


Figure 3. (a) Potential curves of $\Phi_{\text{Al-Si}}$ and $\Phi_{\text{Al-C}}$. (b) AE data from *ab initio* calculation (lines) and pair potentials (scattered symbols).

Table 1. The potential parameters for bulk SiC, where the two-body terms are in Morse potential form ($\Phi(r) = D_0(e^{-2\alpha(r-R_0)} - 2e^{-\alpha(r-R_0)})$) and three-body terms are in MSW potential form.

Two-body terms	C-C	Si-Si	C-Si
D_0 (eV)	1.2349	1.0898	1.0485
α (\AA^{-1})	1.7888	1.4421	1.4675
R_0 (\AA)	2.0066	2.7760	2.4316
Three-body terms	C-Si-C	Si-C-Si	
λ (eV)	4.6929	10.9230	
γ (\AA)	0.2047	0.2047	
$R_{\text{C-Si}}$ (\AA)	3.1832	3.1832	
θ^0	109.47°	109.47°	

where the three-body terms are assigned in MSW form:

$$\Phi_{jik}(r_{ij}, r_{ik}, \theta_{jik}) = \lambda_{jik} \exp\left(\frac{\gamma_{ij}}{r_{ij} - R_{ij}} + \frac{\gamma_{ik}}{r_{ik} - R_{ik}}\right) \times (\cos \theta_{jik} - \cos \theta^0)^2. \quad (4)$$

Because the charge transfer at the interface is mainly confined to the first Al and SiC layers (figure 2), the three-body interaction $j-i-k$ is limited in this region. That means the central atom i is located in the first SiC layer, and j, k are chosen from the neighboring Al and SiC layers. Therefore, six trimers are considered in total: Al-Si-C, Al-Si-Al, Al-C-Si, Al-C-Al, C-Si-C and Si-C-Si.

This potential composition is rather complex, so some assumptions are considered for simplification. First, the equilibrium angles θ^0 of Al-Si-C and Al-C-Si are set to 109.47°, since the central atoms are sp^3 hybridized in the energy-favored interface structures. Second, proper cutoff radii R_{ij} and R_{ik} are chosen to include the nearest-neighbor three-body interactions only. Third, the three interactions $j-i-k$, $j-i-l$ and $i-j-l$ share the same parameter set $\{\gamma_{ij}, R_{ij}\}$. Fourth, the MSW potential parameters for bulk SiC (table 1) [15], which give a good description of some mechanical properties

Table 2. The elastic constants of bulk 3C-SiC, obtained by the interatomic potentials listed in table 1, are in comparison with the *ab initio* and experimental results.

	By potential	<i>Ab initio</i>	Experiment [17]
Bulk modulus (GPa)	231.1	211.3	270
c_{11} (GPa)	414.0	395.5	390
c_{12} (GPa)	139.6	82.7	142
c_{44} (GPa)	196.0	167.1	256

of 3C-SiC (table 2), are adopted by the interfacial C-Si-C and Si-C-Si interactions.

Now we pay attention to the top-site configuration. It is notable that the Al-Si-C (or Al-C-Si for C-terminated interface) angle is equal to 109.47° in this structure. So, due to the first assumption mentioned above, the three-body term Al-Si-C (or Al-C-Si) vanishes. In addition, according to the nearest-neighbor principle (the second assumption), the Al-Si-Al and Al-C-Al terms are also excluded. Thus, the AEs of top-site structures can be expressed as the sum of pair interactions:

$$E_{\text{top-site}}(x) = \sum_{ij} \Phi_{ij}(r_{ij}), \quad (5)$$

where ij is the atom pair across the interface. To derive Φ_{ij} from $E_{\text{top-site}}$ is a regular interfacial adhesion problem, which is solved numerically by a lattice inversion method (refer to the appendix for details).

Comparing with the three-body MSW potential, the functional form of the two-body potential is not predetermined, i.e. it is parameter-free. One can choose appropriate functions for the potential curves plotted in figure 3(a). In this work, the Rahaman-Stillinger-Lemberg (RSL2) potential is used to fit pair potentials

$$\Phi(r) = D_0 e^{\gamma(1-\frac{r}{R_0})} + \frac{a_1}{1 + e^{b_1(r-c_1)}} + \frac{a_2}{1 + e^{b_2(r-c_2)}} + \frac{a_3}{1 + e^{b_3(r-c_3)}}. \quad (6)$$

The resultant potential parameters are listed in table 3.

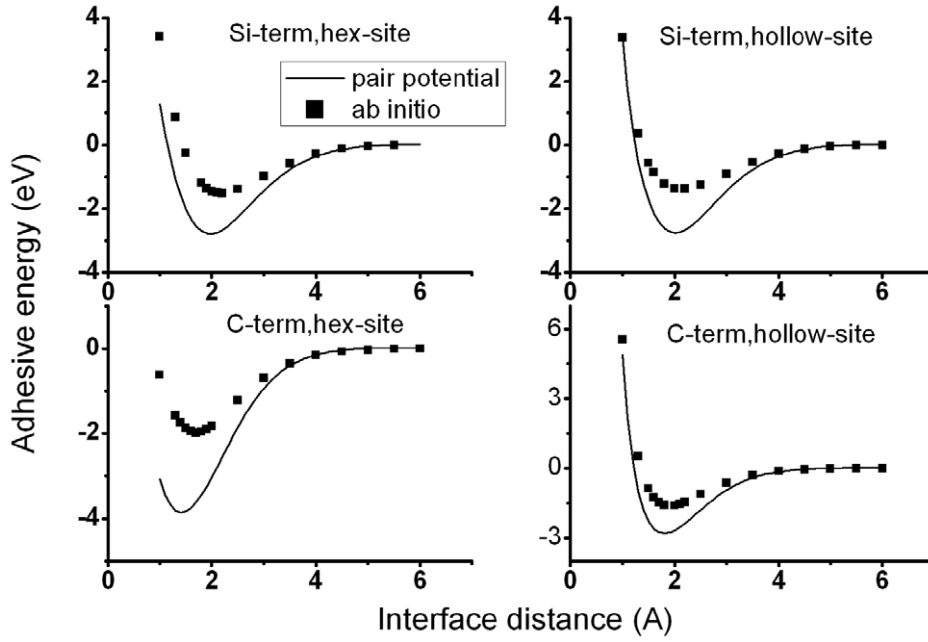


Figure 4. AE data for transferability check, where scattered symbols are *ab initio* results and lines are pair-potential-calculated results. The hex-site and hollow-site structures of Si-terminated and C-terminated interfaces are checked.

Table 3. The pair-potential parameters of $\Phi_{\text{Al-Si}}$, $\Phi_{\text{Al-C}}$ and $\Phi_{\text{Al-Al}}$, fitted in the RSL2 function. Here $\Phi_{\text{Al-Al}}$ for bulk Al is also presented as it will be used in section 3.

	$\Phi_{\text{Al-Si}}$	$\Phi_{\text{Al-C}}$	$\Phi_{\text{Al-Al}}$
D_0 (eV)	68.4853	0.1392	39.3540
R_0 (Å)	1.0	1.0	1.0
y	1.2844	5.7526	2.3528
a_1 (eV)	75.0606	66.9374	-0.6804
b_1 (1/Å)	2.9238	5.7654	0.82633
c_1 (Å)	0.9512	0.9401	2.9120
a_2 (eV)	-12.2142	1.1365	-1.4231
b_2 (1/Å)	3.6486	8.2083	1.6881
c_2 (Å)	1.6732	1.6578	1.6446
a_3 (eV)	-55.5837	-0.6407	0.9604
b_3 (1/Å)	1.3456	2.3362	4.1611
c_3 (Å)	1.4086	2.7657	1.5737

As a basic check of $\Phi_{\text{Al-Si}}$ and $\Phi_{\text{Al-C}}$, figure 3(b) plots the AE curves reproduced by potentials in comparison with the original *ab initio* data. The good agreement shows that the resultant potentials are self-consistent. Furthermore, for a transferability check, figure 4 shows the comparisons between *ab initio* and pair-potential-calculated AEs of hollow-site and hex-site structures. There is a significant deviation between them, so three-body modification is needed.

The next step is to fit MSW parameters for Al-Si-C, Al-Si-Al, Al-C-Si and Al-C-Al trimers. In total there are ten undetermined parameters: $\lambda_{\text{Al-Si-C}}$, $\gamma_{\text{Al-Si}}$, $R_{\text{Al-Si}}$, $\lambda_{\text{Al-Si-Al}}$, $\theta_{\text{Al-Si-Al}}^0$, $\lambda_{\text{Al-C-Si}}$, $\gamma_{\text{Al-C}}$, $R_{\text{Al-C}}$, $\lambda_{\text{Al-C-Al}}$ and $\theta_{\text{Al-C-Al}}^0$. The AE data of the hex-site structure (see figure 1(C)) are employed to determine them. In this structure, the three-body

contribution can be expressed as

$$\begin{aligned}
 E_3^{\text{Si-term}}(x) &= \lambda_{\text{Al-Si-C}} \\
 &\times \exp\left(\frac{\gamma_{\text{Al-Si}}}{\sqrt{x^2 + a_{\text{SiC}}^2/6} - R_{\text{Al-Si}}} + \frac{\gamma_{\text{Si-C}}}{\sqrt{3}a_{\text{SiC}}/4 - R_{\text{Si-C}}}\right) \\
 &\times \left[3 \left(\frac{-2a_{\text{SiC}} - \sqrt{3}x}{3\sqrt{3}\sqrt{x^2 + a_{\text{SiC}}^2/6}} + \frac{1}{3} \right)^2 \right. \\
 &\left. + 6 \left(\frac{a_{\text{SiC}} - \sqrt{3}x}{3\sqrt{3}\sqrt{x^2 + a_{\text{SiC}}^2/6}} + \frac{1}{3} \right)^2 \right] \\
 &+ \lambda_{\text{Al-Si-Al}} \exp\left(\frac{2\gamma_{\text{Al-Si}}}{\sqrt{x^2 + a_{\text{SiC}}^2/6} - R_{\text{Al-Si}}}\right) \\
 &\times 3 \left(\frac{x^2 - a_{\text{SiC}}^2/12}{x^2 + a_{\text{SiC}}^2/6} - \cos(\theta_{\text{Al-Si-Al}}^0) \right) \quad (7) \\
 E_3^{\text{C-term}}(x) &= \lambda_{\text{Al-C-Si}} \\
 &\times \exp\left(\frac{\gamma_{\text{Al-C}}}{\sqrt{x^2 + a_{\text{SiC}}^2/6} - R_{\text{Al-C}}} + \frac{\gamma_{\text{Si-C}}}{\sqrt{3}a_{\text{SiC}}/4 - R_{\text{Si-C}}}\right) \\
 &\times \left[3 \left(\frac{-2a_{\text{SiC}} - \sqrt{3}x}{3\sqrt{3}\sqrt{x^2 + a_{\text{SiC}}^2/6}} + \frac{1}{3} \right)^2 \right. \\
 &\left. + 6 \left(\frac{a_{\text{SiC}} - \sqrt{3}x}{3\sqrt{3}\sqrt{x^2 + a_{\text{SiC}}^2/6}} + \frac{1}{3} \right)^2 \right]
 \end{aligned}$$

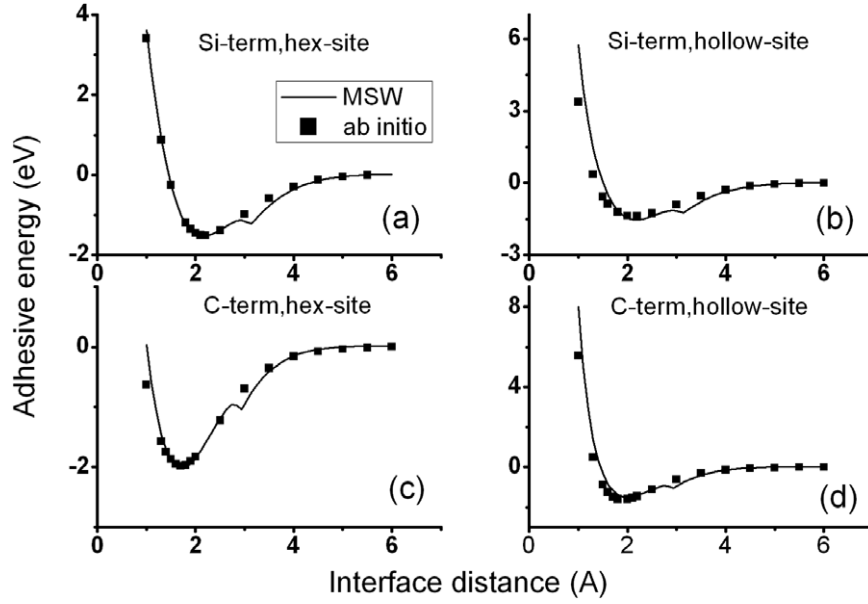


Figure 5. AE data for transferability check again, where scattered symbols represent the results from *ab initio* calculations and lines represent the results from interfacial potentials (including two-body and three-body terms). (a) and (b) are for hex-site and hollow-site structures of the Si-terminated interface, and (c) and (d) are for hex-site and hollow-site structures of the C-terminated interface.

Table 4. MSW three-body potential parameters for Al/SiC(111) interface. λ is in units of eV, γ and R are in units of \AA and θ is in units of degrees.

Al-Si-C and Al-Si-Al	$\lambda_{\text{Al-Si-C}}$	$\gamma_{\text{Al-Si}}$	$R_{\text{Al-Si}}$	$\lambda_{\text{Al-Si-Al}}$	$\theta_{\text{Al-Si-Al}}^0$
	0.9109	0.1878	3.65	0.0342	179.9986
Al-C-Si and Al-C-Al	$\lambda_{\text{Al-C-Si}}$	$\gamma_{\text{Al-C}}$	$R_{\text{Al-C}}$	$\lambda_{\text{Al-C-Al}}$	$\theta_{\text{Al-C-Al}}^0$
	0.3283	0.0584	3.43	0.6229	2.2947

$$\begin{aligned}
 & + \lambda_{\text{Al-C-Al}} \exp \left(\frac{2\gamma_{\text{Al-C}}}{\sqrt{x^2 + a_{\text{SiC}}^2/6} - R_{\text{Al-C}}} \right) \\
 & \times 3 \left(\frac{x^2 - a_{\text{SiC}}^2/12}{x^2 + a_{\text{SiC}}^2/6} - \cos(\theta_{\text{Al-C-Al}}^0) \right) \quad (8)
 \end{aligned}$$

where $E_3^{\text{Si-term}}$ and $E_3^{\text{C-term}}$ are the three-body parts of AE for Si-terminated and C-terminated interfaces, x is the interfacial distance and a_{SiC} is the lattice constant of SiC.

An optimization algorithm is used to find a set of the most satisfactory potential parameters by fitting (7) and (8). The results are listed in table 4. Together with $\gamma_{\text{Si-C}}$ and $R_{\text{Si-C}}$ in table 1, the three-body potentials are finally determined. Figure 5 shows the transferability check again, by considering both the two-body and three-body interactions. The *ab initio* AE data are well reproduced by interfacial potentials, for both hex-site and hollow-site structures. We believe that the three-body modification extends the transferability.

3. Misfit dislocation position

Misfit is an inherent property of a heterophase interface, which may induce misfit dislocations [18, 19]. In a mismatched interface, misfit dislocation usually tends to appear at the

interface plane, i.e. the phase boundary between the two sides. This is the general case, but there are also some exceptions. For example, $\text{Ni}/(\text{Al}_2\text{O}_3)_{\text{Al}}$ has a reconstructed layer on the interface and the misfit dislocation is on the Ni side [20].

So we propose a concept called dislocation position to describe at which layer the dislocation appears. In general, the dislocation position of a film/substrate system is determined by two factors: the adhesive energy across the interface and the misfit-induced elastic energy in the film. At the Al/SiC interface, a rather strong adhesion is found between Al and SiC, which may induce some coherent layers on the interface and eject the misfit dislocation into the Al side. In this condition, atomistic simulations are performed for a quantitative evaluation.

The interface model for the atomistic simulation contains eight Al MLs and thirteen SiC MLs, as shown in figure 6. In order to construct a misfit dislocation, we introduce a mismatch plane in this model, with $(n+1) \times (n+1):n \times n$ atomic ratio between its two sides. For Al/SiC, n is 13 to approach the reciprocal of the misfit. The position of the dislocation is exhibited by the mismatch plane, which is denoted as P in figure 6. For energetic consideration, the unit atomic energy of Al is taken as the criterion, calculated by

$$E_{\text{Al}} = \frac{1}{N_{\text{Al}}} (E_{\text{total}} - E_{\text{SiC}}), \quad (9)$$

where E_{total} is the total energy of the interface system, E_{SiC} is the partial energy of the SiC side and N_{Al} is the number of Al atoms. E_{Al} includes the contributions of interfacial adhesive energy and the elastic energy of the Al lattice. Figure 7 displays the curves of E_{Al} versus P . It shows that E_{Al} reaches its minimum value at $P = 1$, for both Si-terminated and C-terminated interfaces. So there is a coherent Al layer at the

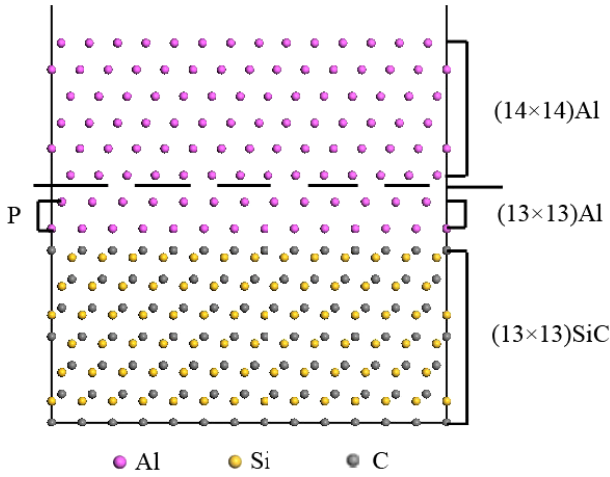


Figure 6. The interface model of Al/SiC(111), where the dashed line indicates the mismatch plane. The $P = 2$ case is illustrated.

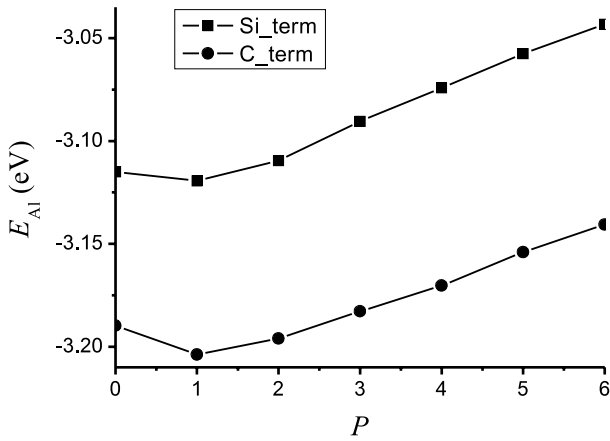


Figure 7. The E_{Al} versus P curves for the Al/SiC(111) interface.

interface and the misfit dislocation is above this layer. This is similar to the Ni/Al₂O₃ case [20].

One may be interested in what role the resultant coherent interlayer plays in determining the interface properties. For this purpose, the cases $P = 1$ and $P = 0$ are compared, denoted as interface _{$P=1$} and interface _{$P=0$} , respectively. It is obvious that interfacial adhesion is affected by this coherent interlayer. The AEs of interface _{$P=1$} are 3.947 (Si-terminated) and 5.572 J m⁻² (C-terminated), while those of interface _{$P=0$} are 3.834 (Si-terminated) and 5.183 J m⁻² (C-terminated). The former ones are relatively larger, indicating that the coherent Al interlayer at the phase boundary protects the adhesion between Al and SiC from being weakened by the misfit dislocation.

Now, the influence of the coherent interlayer on electronic properties is also discussed. As shown in figure 2, the charge transfer at the Al/SiC(111) interface is localized between the first Al and SiC layers. That suggests the electron structure at the interface is mainly determined by the atomic configuration between the first layer Al and SiC. In the $P = 1$ case, the coherent Al interlayer keeps the interfacial configuration homogeneously in the top-site structure. So the misfit dislocation is weakly related to the interfacial

electronic structure as it is above the interlayer and the top-site configuration of the ideal interface is a reasonable approximation for the study of electronic properties.

4. Conclusion

In this work, we derive interfacial potentials for the Al/SiC(111) interface, which are combinations of two-body and three-body interactions, from the *ab initio* calculated AEs. The two-body terms are parameter-free ones obtained by a lattice inversion method, and the three-body terms are in the form of an MSW potential, added as a modification. A series of checks show that these potentials are self-consistent and transferable in some metastable structures, giving a good description of the AE data at six representative interface configurations. So we believe they can support some advanced atomic studies on complex interface structures.

For applications, these potentials are used to study misfit dislocation in the Al/SiC(111) interface. Atomic simulation results show that there is a coherent Al layer on the interface and the misfit dislocation is above this layer. The coherent interlayer is important in affecting the interfacial adhesion and electronic properties.

Acknowledgments

This work is supported by the Nature Science Foundation of China (NSFC no. 50531050) and the 973 project (no. 2006CB605100).

Appendix

Now, we introduce a lattice inversion method for deriving parameter-free interfacial pair potentials from *ab initio* calculated AEs. In this appendix, the AEs of top-site structures (see figure 1(A)) are used, evaluated as a function of interfacial distance x , as shown in figure 3(b). They are denoted as $E_{Si-term}(x)$ and $E_{C-term}(x)$ for Si-terminated and C-terminated interfaces, respectively.

In a pair-potential approach, AEs are equal to the summation of pair interactions across the interface, expressed as

$$E_{X-term}(x) = \sum_{i,j} \Phi_{ij}(r_{ij}), \quad (A.1)$$

where X is Si or C, ij is the atom pair across the interface and r_{ij} is the pair distance.

As there are two potentials Φ_{Al-Si} and Φ_{Al-C} across Al/SiC interface, equation (A.1) can be written as

$$E_{Si-term}(x) = \sum_{r_a} a \Phi_{Al-Si}(r_a(x)) + \sum_{r_b} b \Phi_{Al-C}(r_b(x)), \quad (A.2)$$

$$E_{C-term}(x) = \sum_{r_a} a \Phi_{Al-C}(r_a(x)) + \sum_{r_b} b \Phi_{Al-Si}(r_b(x)), \quad (A.3)$$

where a and b are coordination numbers.

For simplification, some intermediate variables are defined:

$$\begin{aligned} E_{\pm}(x) &= E_{\text{Si-term}}(x) \pm E_{\text{C-term}}(x) \quad \text{and} \\ \Phi_{\pm}(r) &= \Phi_{\text{Al-Si}}(r) \pm \Phi_{\text{Al-C}}(r), \end{aligned} \quad (\text{A.4})$$

and we can get

$$\begin{aligned} E_{\pm}(x) &= \sum_{r_a} a \Phi_{\pm}(r_a(x)) \pm \sum_{r_b} b \Phi_{\pm}(r_b(x)) \\ &= \sum_r p_{\pm} \Phi_{\pm}(r(x)), \end{aligned} \quad (\text{A.5})$$

where p_{\pm} is a synthesis of a and b , and $r(x)$ is a synthesis $r_a(x)$ and $r_b(x)$.

The inverse problem is to solve (A.5) to get $\Phi_{\text{Al-Si}}$ and $\Phi_{\text{Al-C}}$. For this purpose, we use a numerical approach by separating the pair distance r into a series of scattered values: $r_1 < r_2 < \dots < r_n$. And then, for r between r_i and r_{i+1} , $\Phi_{\pm}(r)$ is re-evaluated by an interpolation approximation:

$$\Phi_{\pm}(r) = \frac{r - r_{i+1}}{r_i - r_{i+1}} \Phi_{\pm}(r_i) + \frac{r - r_i}{r_{i+1} - r_i} \Phi_{\pm}(r_{i+1}). \quad (\text{A.6})$$

In this way, equation (A.5) is changed into a linear equation by choosing a series of interfacial distances $x_1 < x_2 < \dots < x_n$:

$$E_{\pm}(x_i) = \sum_{j=1}^n g_{\pm}^{ij} \Phi_{\pm}(r_j). \quad (\text{A.7})$$

For i from 1 to n , the matrix element g_{\pm}^{ij} is derived from p_{\pm} by using (A.6).

Let $e_{\pm} = [E_{\pm}(x_1), E_{\pm}(x_2), \dots, E_{\pm}(x_n)]$ and $\varphi_{\pm} = [\Phi_{\pm}(r_1), \Phi_{\pm}(r_2), \dots, \Phi_{\pm}(r_n)]$. We get

$$e_{\pm} = \varphi_{\pm} G_{\pm}, \quad (\text{A.8})$$

where G_{\pm} is an $n \times n$ matrix with its element $G_{\pm}^{ij} = g_{\pm}^{ij}$. The inverse problem can be solved by calculating the inverse matrix of G_{\pm} :

$$\varphi_{\pm} = e_{\pm} G_{\pm}^{-1}. \quad (\text{A.9})$$

As a result, $\Phi_{\text{Al-Si}}$ and $\Phi_{\text{Al-C}}$ are obtained, as plotted in figure 3(a).

References

- [1] Lu W C, Zhang K M and Xie X D 1992 Adsorption of aluminum on β -SiC(100) surfaces *Phys. Rev. B* **45** 11048
- [2] Hoekstra J and Kohyama M 1998 *Ab initio* calculations of the β -SiC(001)/Al interface *Phys. Rev. B* **57** 2334
- [3] Tanaka S and Kohyama M 2003 *Ab initio* study of 3C-SiC/M (M = Ti or Al) nano-hetero interfaces *Appl. Surf. Sci.* **216** 471
- [4] Kohyama M 1996 *Ab initio* calculations for SiC-Al interfaces: tests of electronic-minimization techniques *Modelling Simul. Mater. Sci. Eng.* **4** 397
- [5] Luo X, Qian G, Wang E G and Chen C 1999 Molecular-dynamics simulation of Al/SiC interface structures *Phys. Rev. B* **59** 10125
- [6] Fan T X, Zhang D, Wu R J, Shibayanagi T and Naka M 2002 Polytropy of SiC and interfacial structure in SiCp/Al composites *J. Mater. Sci.* **37** 5191
- [7] Bermudez V M 1988 Growth and structure of aluminum films on (001) silicon carbide *J. Appl. Phys.* **63** 4951
- [8] Porte L 1986 Photoemission spectroscopy study of the Al/SiC interface *J. Appl. Phys.* **60** 635
- [9] Zhao H Y and Chen N X 2008 Inverse adhesion problem for extracting interfacial pair potentials for the Al(001)/3C-SiC(001) interface *Inverse Problems* **24** 035019
- [10] Stillinger F H and Weber T A 1985 Computer simulation of local order in condensed phases of silicon *Phys. Rev. B* **31** 5262
- [11] Feuston B P and Garofalini S H 1989 Empirical three-body potential for vitreous silica *J. Chem. Phys.* **89** 5818
- [12] Liu Y, Chen N X and Kang Y M 2002 Virtual lattice technique and the interatomic potentials of zinc-blend-type binary compounds *Mod. Phys. Lett. B* **16** 187
- [13] Liu Y, Kang Y M and Chen N X 2003 *Ab initio* interatomic potentials for cubic boron nitride *J. Alloys Compounds* **349** 17
- [14] Vashishta P, Kalia R K, Nakano A and Rino J P 2007 Interaction potential for silicon carbide: a molecular dynamics study of elastic constants and vibrational density of states for crystalline and amorphous silicon carbide *J. Appl. Phys.* **101** 103515
- [15] Liu Y 2002 *PhD Thesis* Beijing University of Science and Technology
- [16] Milman V, Winkler B, White J A, Pickard C J, Payne M C, Akhmatkaya E V and Nobes R H 2000 Electronic structure, properties, and phase stability of inorganic crystals: a pseudopotential plane-wave study *Int. J. Quantum Chem.* **77** 895
- [17] Feldman D W, Parker J H, Choyke W J and Patrick L 1968 *Phys. Rev.* **173** 787
- [18] Mizoguchi T, Sasaki T, Tanaka S, Matsunaga K, Yamamoto T, Kohyama M and Ikuhara Y 2006 Chemical bonding, interface strength, and oxygen K electron-energy-loss near-edge structure of the Cu/Al₂O₃ interface *Phys. Rev. B* **74** 235408
- [19] Long Y, Chen N X and Wang H Y 2005 Theoretical investigations of misfit dislocations in Pd/MgO(001) interfaces *J. Phys.: Condens. Matter* **17** 6149
- [20] Long Y and Chen N X 2008 Interface reconstruction and dislocation networks for a metal/alumina interface: an atomistic approach *J. Phys.: Condens. Matter* **20** 135005